Available online at www.sciencedirect.com

ScienceDirect

Solar Energy 129 (2016) 297–309

SOLAR ENERGY

www.elsevier.com/locate/solener

Monitoring and rendering of visual and photo-biological properties of daylight-redirecting systems

A. Borisuit [a,*], J. Kämpf [a], M. Münch [a,b], A. Thanachareonkit [c], J.-L. Scartezzini [a]

[a] Solar Energy and Building Physics Laboratory (LESO-PB), Ecole Polytechnique Fédérale de Lausanne (EPFL), CH-1015 Lausanne, Switzerland
[b] Group Sleep Research & Clinical Chronobiology, Institute of Physiology, Charité University Medicine Berlin, Germany
[c] Windows and Envelope Materials, Energy Technologies Area, Lawrence Berkeley National Laboratory, USA

Received 6 March 2015; received in revised form 3 August 2015; accepted 2 December 2015

Communicated by: Associate Editor Beltran Liliana Beltran

Abstract

We previously developed a Camera-Like Light Sensor (CLLS) to record images using a novel High Dynamic Range (HDR) imaging vision sensor. The device was equipped with customized filters for adapting the camera's spectral sensitivity to both photopic and circadian sensitivities. Here, we aim at investigating photometric and circadian metrics to assess and simulate the potential of light on non-visual functions. The CLLS was used to monitor luminance and circadian weighted radiance (L_{ec}) over time in two test rooms, equipped with different daylight re-directing devices: venetian blinds (VB) and optical louver systems (OLS). Additionally, a computer simulation was performed for the two test rooms using the software RADIANCE: false colour images were used to demonstrate distribution of luminance and absolute values of L_{ec}. Circadian weighted irradiance (E_{ec}) was also computed at different positions corresponding to the gaze directions of a seated office worker. From our results, the VB provided overall higher illuminance compared to the OLS, but when a virtually seated observer was facing desk, the OLS provided larger circadian weighted irradiance in the afternoon. Our results illustrate the use of simulations for circadian metrics, which will be applicable in the future to predict the potential impact of light on non-visual functions for daylighting optimization in buildings.

Keywords: Non-visual effects; Camera-Like Light Sensor (CLLS); Monitoring; Simulation; Daylighting systems

1. Introduction

Lighting simulations are deployed during the early building design phase in order to ensure sufficient indoor lighting availability and quality for visual purposes. Physically-based rendering programs for computer simulations have been widely used for that purpose, such as RADIANCE which is applied based on as a backward ray tracing technique (Larson and Shakespeare, 1998). The simulation results obtained with RADIANCE are considered to be accurate for daylighting assessments (Maamari et al., 2003; Mardaljevic, 1999; Ulbricht et al., 2005; Thanachareonkit, 2008) and annual daylight simulations can be performed in order to predict the annual distribution of daylight provision for buildings mounted with different daylighting systems (Reinhart and Herkel, 2000; McNeil and Lee, 2013; Nabil and Mardaljevic, 2005).

Abbreviations: CLLS, Camera/Like Light Sensor; E_{ec} (W/m^2), circadian weighted irradiance; L_{ec} (W/m^2 sr), circadian weighted radiance; VB, venetian blinds; OLS, optical louver systems; HDR, High Dynamic Range.

* Corresponding author.

http://dx.doi.org/10.1016/j.solener.2015.12.052
0038-092X/

To optimize daylighting strategies in buildings, several daylighting metrics and photometric variables are used to assess indoor lighting conditions. Most of the lighting criteria aimed at complying with requirements for related visual tasks. It is also known that besides visual aspects, light also influences circadian, physiological and behavioural effects in humans: the so-called "photobiological" or non-visual effects of light. Many lighting properties have an influence on occupants' physiology and behaviour, for example on mood, alertness, health and well-being (Cajochen, 2007; Chellappa et al., 2011; CIE, 2004; Münch et al., 2012; Münch and Bromundt, 2012; Rea et al., 2008; Wirz-Justice and Fournier, 2010). In order to account more specifically for these non-visual effects of light, appropriate metrics must be used to assess when measuring light.

Photometric variables are commonly used to assess the light properties in the visible range, i.e. from 380 to 780 nm; they are weighted by the sensitivity of rods and cones for humans, according to the CIE luminous efficiency function or $V(\lambda)$ curve (CIE, 1978). On the other hand, the circadian sensitivity function or $C(\lambda)$ curve was introduced in order to assess light properties important for impacting on the non-visual effects of light (Gall and Bieske, 2004; Thapan et al., 2001; Brainard et al., 2001). The $C(\lambda)$ curve is based on the relative sensitivity by a new class of photoreceptors located in the retinal ganglion cells, the so-called intrinsically photosensitive retinal ganglion cells (ipRGC) (Lucas et al., 2014). The ipRGCs are known to convey many non-visual functions such as circadian rhythms, the pupil light reflex, and hormonal secretion (Lewy et al., 1980; Cajochen et al., 2005; Lucas et al., 2001; Foster, 1998; Czeisler et al., 1986). Prior research showed larger nocturnal melatonin suppression in humans with narrow-bandwidth blue light (446–477 nm) (Thapan et al., 2001; Brainard et al., 2001), indicating that melatonin suppression is an indirect sensitivity marker of ipRGCs function. A few research groups have already suggested circadian sensitivity curves (Gall, 2002; Rea, 2002; Bellia and Bisegna, 2013; Kozakov et al., 2008) based on melatonin suppression data in humans, first published by Brainard et al. (2001) and by Thapan et al. (2001). Recently, a few novel devices have been developed for measuring light fluxes in circadian metrics based on the existing circadian sensitivity curves (Bierman et al., 2005; Figueiro et al., 2013; Hubalek et al., 2006).

In two previous publications (Borisuit et al., 2013; Borisuit, 2013), we introduced a Camera-Like Light Sensor (CLLS) to monitor the distribution of circadian weighted radiance (L_{ec}) (Gall and Lapuente, 2002). The key advantage of the CLLS is its great acquisition of speed performance (Borisuit et al., 2012). With customized filters, the CLLS was adapted to the spectral sensitivity of human eyes expressed by the $V(\lambda)$ function according to CIE (CIE, 1978) as well as to the $C(\lambda)$ function, introduced by Gall (2002). The CLLS was used to assess luminance and L_{ec} distribution over time in realistic office spaces, and was used in an experiment with human subjects for visual comfort assessments a working day (Borisuit et al., 2013, 2012; Borisuit, 2013).

Beyond measurements on circadian metrics, a few authors have previously reported lighting simulations with respect to the human circadian system. Geisler-Moroder and Dür (2010) presented the distribution of circadian action factor a_{cv}, the ratio between $C(\lambda)$) and $V(\lambda)$ values for office lighting conditions, obtained using RADIANCE. Pechacek et al. (2008) proposed a method to assess the circadian efficacy of a given light source (such as daylight) by multiplying the known relative radiometric spectrum with an assumed $C(\lambda)$ curve in order to provide a "circadian-equivalent" lux [unit: W-C(λ)] of the light source. Minimum and maximum "circadian-equivalent" illuminance thresholds were considered as "benchmark" for non-visual aspects of each light source (mainly for daylight as D55, D65 or D75) (Andersen et al., 2011); the threshold values were used in DAYSIM, a computer software based on RADIANCE, in order to predict alerting levels as a proxy of health with respect to light spectrum, intensity and timing of light.

In this study, we investigated the distribution of circadian weighted radiance in two test rooms equipped with different daylight-redirecting systems. The CLLS was used to monitor circadian weighted radiance. Additionally, several lighting simulations of the two test rooms were performed; circadian weighted radiance of the test rooms was also computed and compared with the CLLS monitoring results. Firstly, computer models of two test rooms mounted with different daylighting systems were built and the photometric variables of the two models were compared with physical measurements. Secondly, the luminance and luminance ratio of the models were compared with the images obtained by the CLLS equipped with $V(\lambda)$ filters. A comparison of the distribution of L_{ec} (rendered by simulation) with data monitored by the CLLS equipped with $C(\lambda)$ filters was then carried-out. Lastly, the two different daylighting systems were investigated and qualitatively compared.

The computer simulations carried out in this study followed the RGB approximations method by using RADIANCE, as suggested by Geisler-Moroder and Dür (2010). This study targeted to use absolute values of circadian weighted radiance and irradiance. This is not the same procedure as in previous studies where the circadian stimulus, (= the ratio of $C(\lambda)$ and $V(\lambda)$ values Geisler-Moroder and Dür, 2010) and the "circadian-equivalent" lux were investigated (Pechacek et al., 2008; Andersen et al., 2011, 2013). Circadian weighted irradiance was used to compare the potential of a certain light source for non-visual effects provided by two different daylighting systems. This study also served to confirm the reliability of daylighting simulations to assess circadian metrics. For this purpose, we compared the simulations with our CLLS monitoring over time. The daylight flux reproduced by the simulation was determined at different positions in the rooms and over time, in order

to identify the influence of the indoor lighting environment on non-visual aspects. Taken together this study aimed to show: Firstly, the comparisons between monitoring and simulation of the photometric impact of two daylight-redirecting systems on a virtual observer. Secondly, a potential circadian metric of (day)light on a virtual observer at different locations within the test rooms in the course of a sunny day.

2. Methodology

2.1. Monitoring procedure

2.1.1. Camera-Like Light Sensor (CLLS)

The Camera-Like Light Sensor (as shown in Fig. 1a) was used to monitor light fluxes during the day. The original camera "IcyCAM" was initially developed by the Centre Suisse d'Electronique et de Microtechnique (CSEM; Neuchâtel Switzerland). The essential elements of this device are the intra-scene dynamic range (Arm et al., 2008), which allows one single High Dynamic Range (HDR) image to be taken with much higher speed than the classical HDR technique using a conventional CCD camera (Pangaud, 2011).

The CLLS was calibrated for spectral sensitivity and equipped with the appropriate filters in order to adapt the device's spectral sensitivity to the relative sensitivity of the human eye. The spectral sensitivity of the CLLS was assessed using narrow bandwidth monochromatic light beams and a reference light source as described in previous papers (Borisuit et al., 2013, 2012); it was adapted to both photopic $V(\lambda)$ and circadian sensitivity functions $C(\lambda)$. Equipped with customized filters, the spectral sensitivity curve of the CLLS is shown in Fig. 1b and c.

The CLLS was mounted with a fish-eye lens in order to extend its opening angle and be closer to the human visual field ($\sim$120° × 120° for the panorama (Roulet, 2008; Boff and Lincoln, 1988); the vignetting effects (light fall-off at the edge of the image) was also corrected (Borisuit et al., 2012).

During the monitoring process, the CLLS was used to capture images at different times and different positions (see Section 2.1.2). The device was equipped either with $V(\lambda)$ or $C(\lambda)$ correcting filters before the snapshots; it took about two min to change the filters between two recordings.

2.1.2. Experimental setup

The experiments took place on August 24, 2012 in the Advanced Windows Testbed facility of Lawrence Berkeley National Laboratory (LBNL) at Berkeley, California, USA (latitude 37°4′N, longitude 122°1′W). The facility consisted of three identical side-by-side test rooms. In this experiment, two test rooms adjacent to each other were chosen. In Room I, the South-facing interior clerestory window was mounted with VB. In Room II, the South-facing interior clerestory window was mounted with OLS. To eliminate the effect of the daylight window and to focus only on the effects of the daylight re-directing system, the lower daylight windows were blocked with the blackout curtains, all possible light leakages were sealed.

Photometric monitoring was carried at the two locations in each room (Fig. 2): the sensor position A faced the desk and a PC; sensor position B faced the window. Both positions were located 1.2 m above the floor to represent the approximate eyes' level of a sitting person. Sets of images were taken at 9 AM, 12 PM and 3 PM (Pacific Daylight Time; PDT), under clear sky conditions.

A few other physical measurements were also carried out, including the outdoor solar irradiance and the indoor illuminance. Both variables were recorded all day long at 1-min intervals by using the National Instruments (NI) LabView data acquisition software. Global horizontal and direct normal irradiance at the rooftop as well as the south vertical irradiance were monitored by using pyranometers (Hukseflux DR01 and SR12, Delft, the Netherlands, and LI-COR Li-200, Nebraska, USA). Indoor vertical illuminance at position A and B (shown in Fig. 2) was recorded using Lux-meters (Li-Cor; LI-210SA, Nebraska, USA).

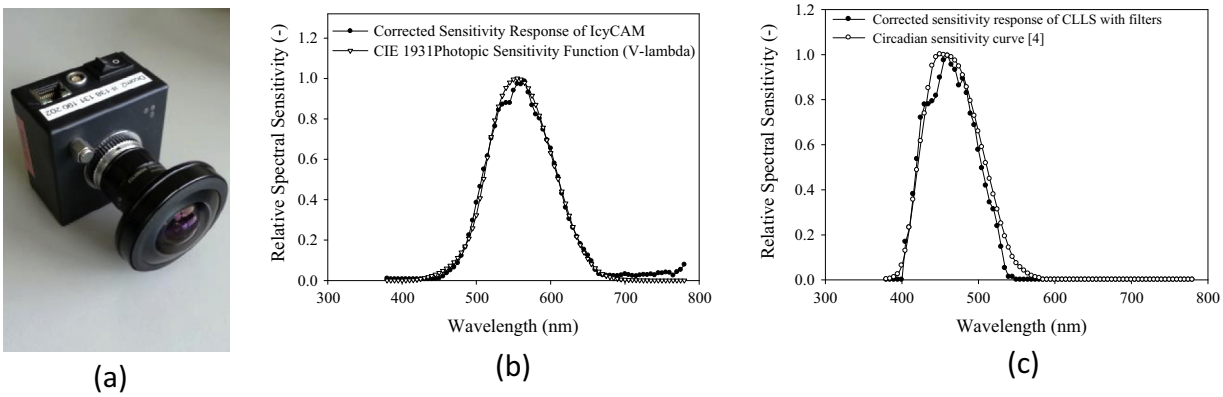

Fig. 1. (a) The CLLS mounted with a fisheye lens; (b) corrected sensitivity response of the CLLS with $V(\lambda)$ filters comparing to the standard photopic sensitivity function and (c) corrected sensitivity response of the CLLS with $C(\lambda)$ filters comparing to the circadian sensitivity function by Gall and Bieske (2004).

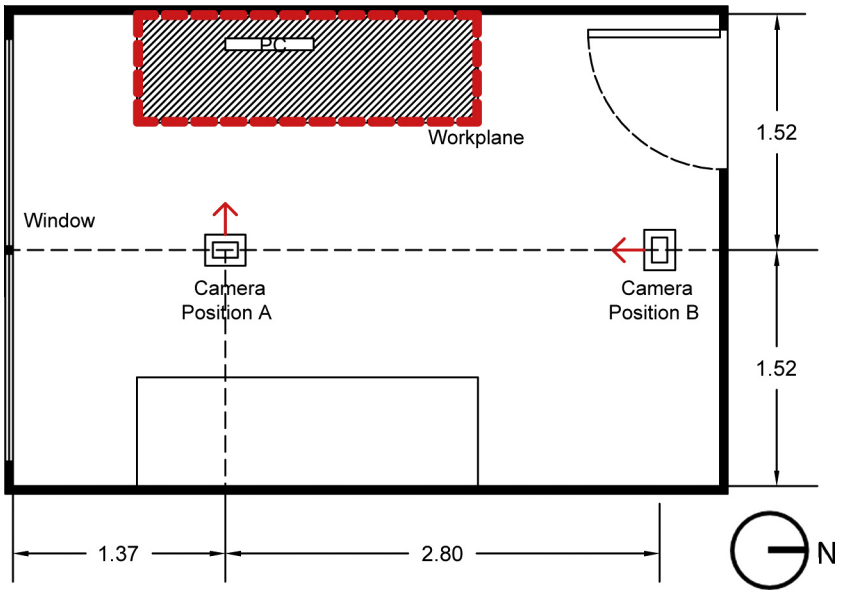

Fig. 2. Experimental setup comprising the positions of the camera and Lux-meters located at the approximate eyes level of a virtual observer (1.2 m above ground). The red arrows indicate the direction of the fish eye lens. For interpretation of the references to colour in this figure legend, the reader is referred to the web version of this article.

2.2. Ray tracing simulations

The RADIANCE simulation software (Larson and Shakespeare, 1998) was used to carry-out daylighting simulations within the two test rooms at different moments. Firstly, the sky luminance distribution of that day (e.g. the 24th August 2012) was generated for clear sky conditions. A clear sky luminance distribution, based on a CIE standard sky, was generated as a virtual sky model using the *gensky* command in RADIANCE; options −B and −R indicating the use of monitored horizontal diffuse irradiance and direct solar irradiance in the software were employed.

The geometrical model of the test rooms was provided by the LBNL Window group and used for the RADIANCE simulations. The daylight-redirecting systems were modelled within RADIANCE using Bidirectional Scattering Distribution Functions (BSDF) (Ward et al., 2011; Kämpf and Scartezzini, 2011). The corresponding BSDF data (stored as XML files) were created using WINDOW 7.2 (LBNL), a software for modelling shading and glazing systems. The test room conditions are listed in Table 1. More details of the test rooms equipped with VB and OLS can be found in Thanachareonkit et al. (2013) and McNeil and Lee (2013), respectively.

Visualisations of both rooms were achieved using RADIANCE according to the parameters shown in Table 2. Fig. 3 presents the rendered images of both rooms compared with images captured by the CLLS.

Photometric quantities were calculated using the *rtrace* and *rcalc* commands in RADIANCE. Three channels corresponding to the red, green and blue (RGB) parts of the visible spectrum are considered in the software to determine radiance values within rendered scenes. The following equation (1) is used to calculate photometric variables, such as luminance and illuminance values in RADIANCE (Larson and Shakespeare, 1998).

$$L = k * (0.265 * R + 0.67 * G + 0.065 * B) \quad (1)$$

For photometric evaluations, the constant k is equal to 179 lm/W corresponding to the "white luminous efficacy" of white light over the visible spectrum (Larson, 1991). R, G and B are value of radiance in W/m^2 sr when luminance is considered and irradiance in W/m^2 when illuminance is considered.

Table 1
Properties of the test rooms and the daylight-redirecting systems.

Element	Room I (with VB)	Room II (with OLS)
Glazing	Double glazed insulated units	Double glazed insulated units
Visible transmission (T_{vis})	0.62	0.62
Shading	25 mm wide matt-white slats with 20 mm spacing 25° adjusted, fully lowered	Matt grey specular louvers reflective film applied on concave-upper louver
Wall reflectance	0.65	0.65
Ceiling reflectance	0.82	0.82
Floor reflectance	0.23	0.23

Table 2
RADIANCE parameters for simulations and renderings of the test rooms.

RADIANCE parameters		Value
−ab	Ambient bounces	7
−aa	Ambient accuracy	0.1
−ad	Ambient divisions	5218
−as	Ambient subdivisions	128
−dt	Direct threshold	0
−ds	Direct source division	0.05
−dc	Direct certainty	1
−dj	Direct jittering	0.7

The circadian weighted radiance (L_{ec}) and irradiance (E_{ec}) can be determined using a similar RGB approximation. Adapted from the formula of Geisler-Moroder and Dür (2010), the following coefficients can be used to approach the circadian sensitivity function by RGB approximations:

$$L_{ec} = k' * (-0.0346 * R + 0.232 * G + 0.558 * B) \quad (2)$$

The constant k' for the circadian metrics considered in this study is equal to 0.23. In the same manner as the white luminous efficacy for photometric response, it was approximated by an average of the relative spectral response of the $C(\lambda)$ function by Gall (2002) over the visible spectrum.

2.3. Comparison of monitored and simulated metrics

The comparisons between monitored and simulated metrics were performed using the following four variables:

2.3.1. Luminance distribution by false colour images

The *Falsecolor* command in RADIANCE was used to create false colour renderings for lighting analysis (Larson and Shakespeare, 1998). Luminance is displayed by using a linear scale ranging from 0 to 200 cd/m^2 in order to visualize its distribution in the test rooms.

2.3.2. Workplane luminance

The average workplane luminance was assessed as the location shown in Fig. 2. The desk shape was defined by creating a mask in an image processing software; the average luminance of the masked area were computed using PHOTOSHOP® and the *pvalue* function of RADIANCE (Borisuit et al., 2010).

2.3.3. Luminance ratio

The luminance of the workplane (considered as task area) and its adjacent surroundings were extracted in the same way. The ratio between the luminance of the different planes was determined and used for different comparisons. According to the IESNA guidelines for luminance ratios between surfaces located in the field of view, a maximum contrast of 1:3 is permitted between the task area and the adjacent surroundings (Rea, 2000).

2.3.4. Circadian weighted radiance distribution by false colour images

Similar to luminance distribution, circadian weighted radiances (L_{ec}) were displayed using false colour images. *Pcomb* command in RADIANCE was used for the rendering of circadian metrics, Eq. (2) being used as new RGB coefficients (instead of Eq. (1) for photometry).

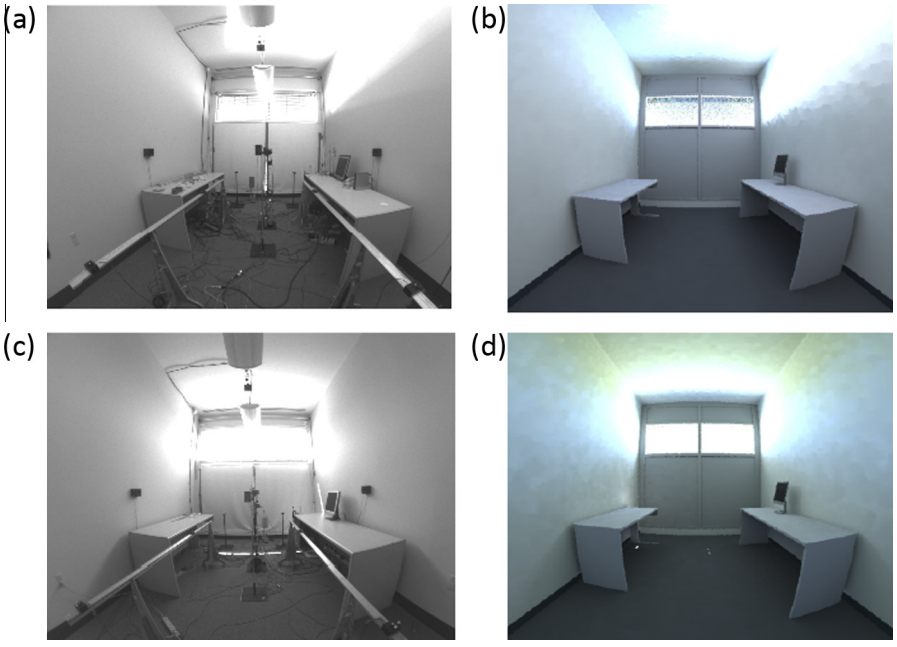

Fig. 3. (a) Images of the test room with OLS captured by CLLS and (b) rendered by RADIANCE simulations; (c) images of the room with VB captured by CLLS and (d) rendered by RADIANCE simulations.

3. Results

3.1. Empirical validation of simulations

The virtual models of the two test rooms were empirically validated by comparing the simulated photometric variables with the monitored data. The global horizontal irradiance and the vertical irradiance were compared first with on-site data monitoring in order to validate the sky models generated by the *gensky* command (as described in Section 2.2). The sky models provided respectable outdoor irradiances since the relative errors were between 0% and 10.8%.

Secondly, in order to corroborate the indoor luminous distribution, the vertical illuminance at the CLLS's position (facing the windows and/or the desk) was calculated from hourly recordings using the computer models. Vertical illuminance was then compared to the monitored data using a Lux-meter, as shown in Fig. 4. The simulated horizontal illuminances of the scene facing the window were comparable to the monitored data. The simulated illuminances of the scene facing the desk were less accurate; the largest relative error reached 54% for the OLS at 11 AM. However, monitored and simulated data remain comparable, since there was no significant difference between illuminances monitored using the CLLS and those simulated with RADIANCE (*t*-test for independent samples; $p = 0.74$).

Overall, VB provided higher illuminance (averaged from simulations and monitored data) when compared to OLS [2-way Analysis of Variance; ANOVA; with the factors 'condition' (VB vs. OLS) × 'position' (A vs. B); main effect of 'condition'; $p < 0.001$; $F_{1,30} = 97.84$], but there was a significant interaction with the factors 'condition' and 'position' ($F_{1,30} = 5.53$; $p = 0.025$), such that only with VB, there was a difference between the two positions in the room. With VB, illuminance was higher at position B (=facing the windows), when compared to position A (=facing the desk; Duncan's multiple range test). This indicates that the OLS provided a more even illuminance distribution also deeper in the room, even though it provided less illuminance.

3.2. Analysis of luminance distribution

3.2.1. Comparison of luminance distribution using false colour images

Luminance distributions in the two test rooms were determined using RADIANCE. The distributions observed for the facing-desk scene are presented in false colour images in Fig. 5. Colour bars on the left side represent how much luminance is incident on the horizontal and vertical planes; yellow represents the highest (200 cd/m^2) and violet represents the lowest luminance (0 cd/m^2). The first group of images corresponds to Room I (with VB; Fig. 5a): the second group of images shows Room II, with an OLS (Fig. 5b). The first columns of each group present the images captured by the CLLS, the second columns show the images generated by computer simulation. The first, the second and the last row show the images rendered at 9 AM, 12 PM and 3:00 PM, respectively. Overall, the simulation provided renderings which were qualitatively comparable (from visual inspection) to the CLLS images acquired on the same day (August, 24) at 9 AM and 12 PM for both test rooms, but with slightly higher luminance at 3:00 PM, especially for the room with OLS.

3.2.2. Comparison of workplane luminance

For further quantitative analysis, the luminance at the work plane (see Fig. 2) was extracted from monitored and simulated images, as shown in Table 3a. The differences between the desktop luminance ranged from 10.4 to

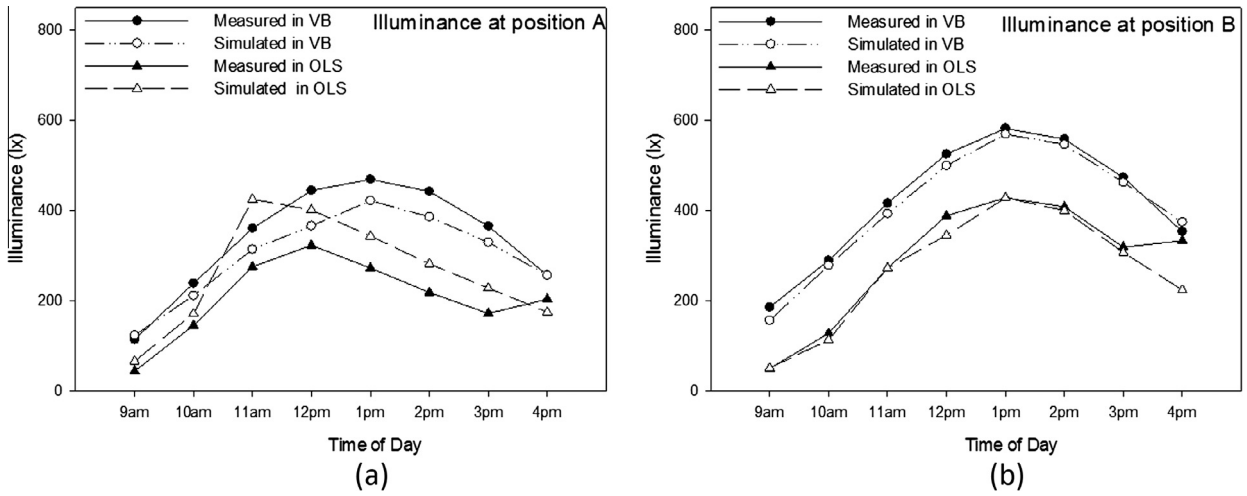

Fig. 4. Measured (solid lines and black symbols) and simulated illuminance (dashed lines and white symbols) for both test rooms: (a) Illuminance at the position A (facing the desk) and (b) Illuminance at the position B (facing the window).

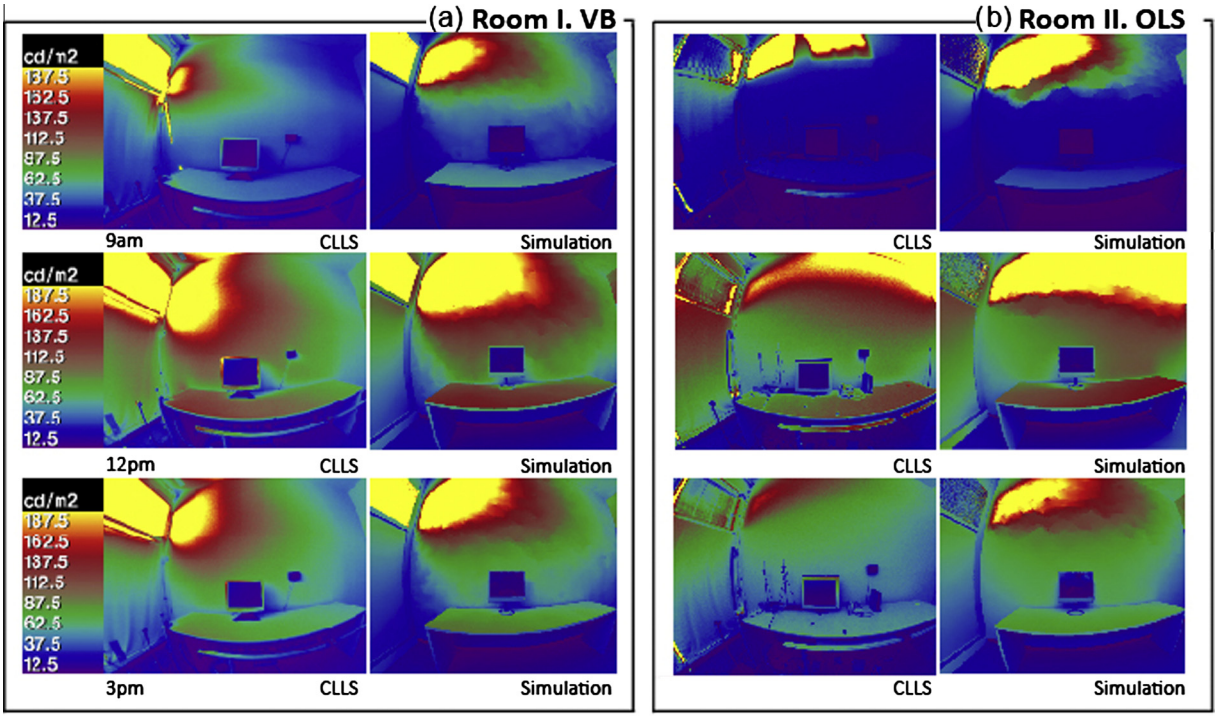

Fig. 5. Luminance distribution from both rooms with views facing window presented in false colour images for: (a) Room I with VB at 9 AM, 12 PM and 3:00 PM captured by the CLLS and simulated with RADIANCE; (b) Room II with OLS at 9 AM, 12 PM and 3:00 PM captured by the CLLS (column 1 and 3) and simulated with RADIANCE (columns 2 and 4).

Table 3
Luminance (cd/m^2) monitored with the CLLS, as well as simulated with Radiance on the: (a) work planes (desk), as well as: (b) luminance ratio between desk and walls.

Time	Elements	OLS			VB		
		CLLS	Simulation	Difference	CLLS	Simulation	Difference
9AM	(a) Desk	21.8	32.2	10.4	38.4	46.7	8.3
	(b) Ratio desk: wall	1:3.3	1:3	–	1:1.5	1:1.6	–
12PM	(a) Desk	90.7	114.5	23.8	95.9	108.7	12.8
	(b) Ratio desk: wall	1:1.5	1:1.3	–	1:1.2	1:1.4	–
3:00PM	(a) Desk	48.7	68.1	19.4	68.4	73	4.6
	(b) Ratio desk: wall	1:1.3	1:1.4	–	1:1.3	1:1.4	–

23.8 cd/m^2 for the OLS, and from 4.6 to 12.8 cd/m^2 for the VB. The differences were higher in the test room with OLS, even though VB provided higher luminance.

3.2.3. Comparison of luminance ratio between the desktop and surroundings

The luminance ratio between the desk (= work plane) and its surrounding was determined in order to compare the luminance distribution in the rooms. This ratio is generally used to describe visual comfort (Rea, 2000). The luminance of the desk adjacent the wall (a) was also extracted as shown in Table 3; (b) shows the corresponding ratio between the work plane and wall luminance (as an adjacent surrounding) in the morning, at noon and in the afternoon. Those ratios did not exceed 1:3, which is recommended for visual comfort by IESNA (Rea, 2000).

3.3. Analysis of circadian weighted radiance

3.3.1. Comparison of circadian weighted radiance distribution

In the next step, we compared the distribution of circadian weighted radiance (L_{ec}) according to the $C(\lambda)$ circadian sensitivity function monitored with the CLLS, with those obtained by computer simulations (Fig. 6). False colour images were rendered for the window facing views in order to outline the L_{ec} distribution in the entire rooms.

The computer simulations generated L_{ec} distributions seemed comparable to those monitored with the CLLS (from visual inspection; Fig. 6a and b). Both daylighting systems provided lower L_{ec} values in the morning compared to noon and in the afternoon. In the room with VB, some light scattering and shades could be observed

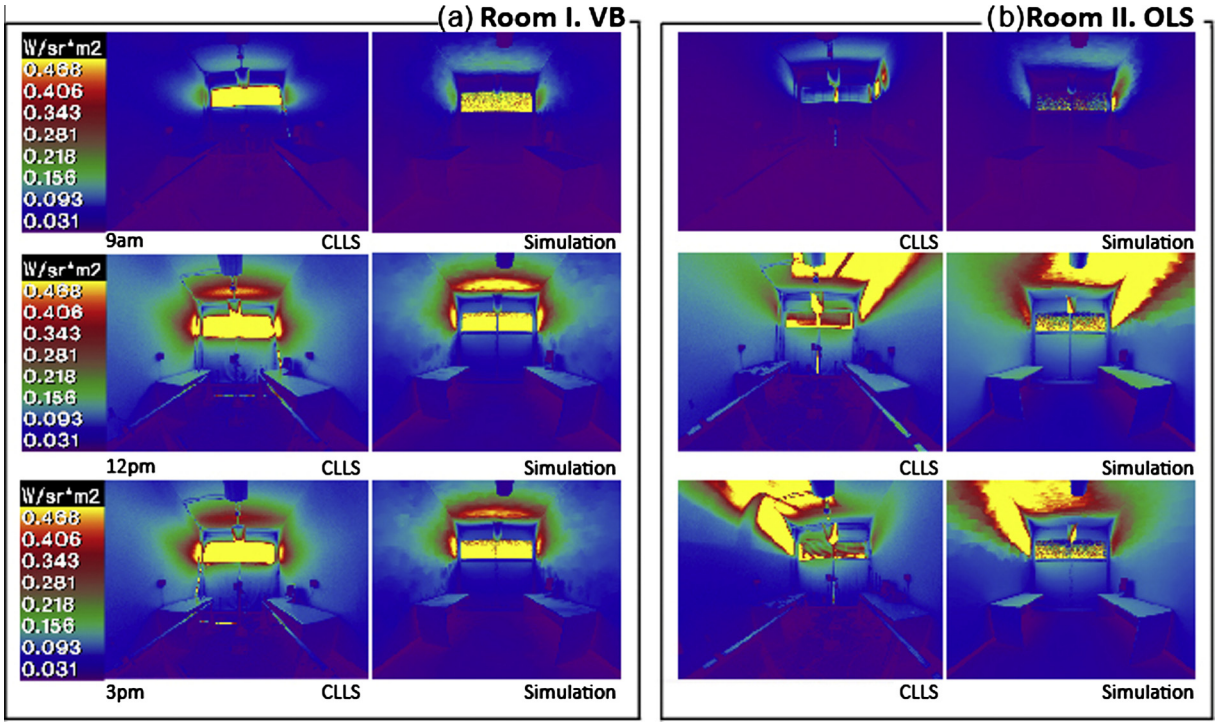

Fig. 6. Rendered views facing the window are presented in false colours for circadian weighted radiance L_{ec} (a) Room I equipped with VB at 9 AM, 12 PM and 3:00 PM captured by the CLLS and simulated with *RADIANCE*; (b) Room II equipped with OLS at 9 AM, 12 PM and 3:00 PM, captured by the CLLS and simulated with RADIANCE. The left scale represents L_{ec} values of the different room surfaces; yellow corresponds to the highest value (with a maximal circadian weighted radiance of 0.5 W/sr m^2). For interpretation of the references to colour in this figure legend, the reader is referred to the web version of this article.

on the wall underneath the venetian blinds, possibly due to little light gaps between the blinds and the windows in the computer model. For OLS, in the afternoon, the simulations indicated slightly larger L_{ec} on the working plane than those monitored with the CLLS on the horizontal plane (from visual inspection). It might be possible that the simulations accounted for a larger daylight flux into the room in the afternoon, as shown in Fig. 5.

3.3.2. Circadian weighted irradiance at different room positions

To account for circadian metrics, we investigated the daylight flux reaching the eye of a potential virtual observer. The light exposure was accordingly computed and measured using the circadian weighted irradiance (E_{ec}). The sensors were placed for a virtual seated observer (with an approximate height at the eyes of 1.2 m above the ground) at different positions in the room at a distance of 1–4 m from the south window and/or facing the desk and PC (Fig. 7).

The E_{ec} at each position and time of day was calculated by simulations, using the RGB approximations, as described in Section 2.2 and the results are shown in Fig. 8.

An interaction between the three factors 'condition (VB vs. OLS) × 'position' (facing desk vs. facing window) × distance' (1–4 m) was found ($F_{3,84} = 5.14$; $p = 0.003$). Post-hoc tests showed that the room with VB provided significantly larger E_{ec} for a seated virtual observer facing the window at the distance between 2–4 m from the window, when compared to a virtual observer who is facing the window (post hoc analysis; Duncan´s multiple range test; Fig. 9a). These differences were not significant for the room with OLS (Fig. 9b).

Next, the non-visual potential of daylight for an office worker in those rooms was simulated. Therefore, the virtual observer was supposed to be seated facing the lateral walls (or desk and PC), in order to avoid glare, induced by the windows. The circadian weighted irradiance (E_{ec}) values at the eye level of an virtual observer facing the desk were determined at different distances from the window during working hours (from 9 AM to 4 PM; Fig. 10). From visual inspection of the 3-D mesh plots, the VB provided larger E_{ec} near the window at midday; then the E_{ec} decreased gradually along the depth of the room (on average by 76%) and over time (on average by 200%). For the OLS, the E_{ec} values did not decrease much over relative to the distance from the window (on average by 62%); however, the E_{ec} values varied in an extremely large range through the day (at maximum by 461%). The E_{ec} values were low from 9 to 10 AM which correspondences to the low illuminance in the morning, as shown in Fig. 4.

The simulated E_{ec} values of both daylight-redirecting systems were statistically compared hourly for a virtual observer facing the desk (Fig. 11); larger E_{ec} was found in the room equipped with OLS compared to the room with VB between 11 PM and 12 PM (ANOVA; interaction

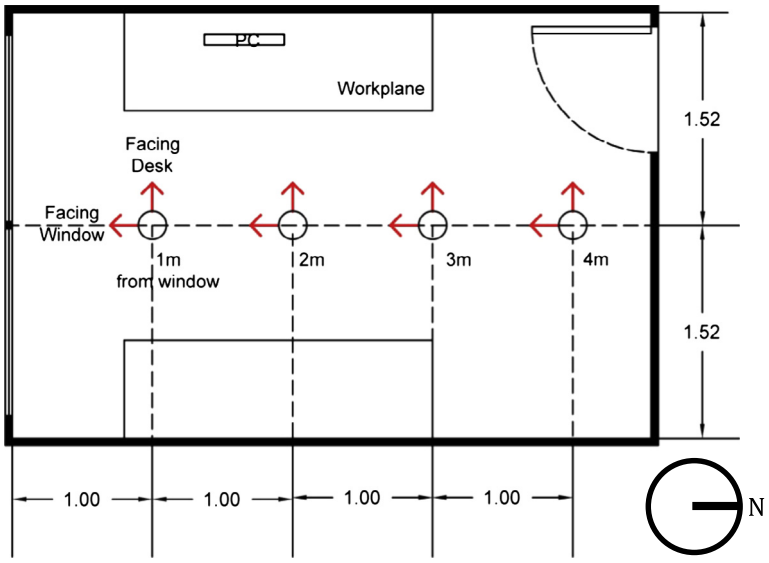

Fig. 7. Simulation positions and gaze directions at the approximate eye level of a seated virtual observer in the test rooms, facing the window or the desk at different distances from the wall (red arrows). For interpretation of the references to colour in this figure legend, the reader is referred to the web version of this article.

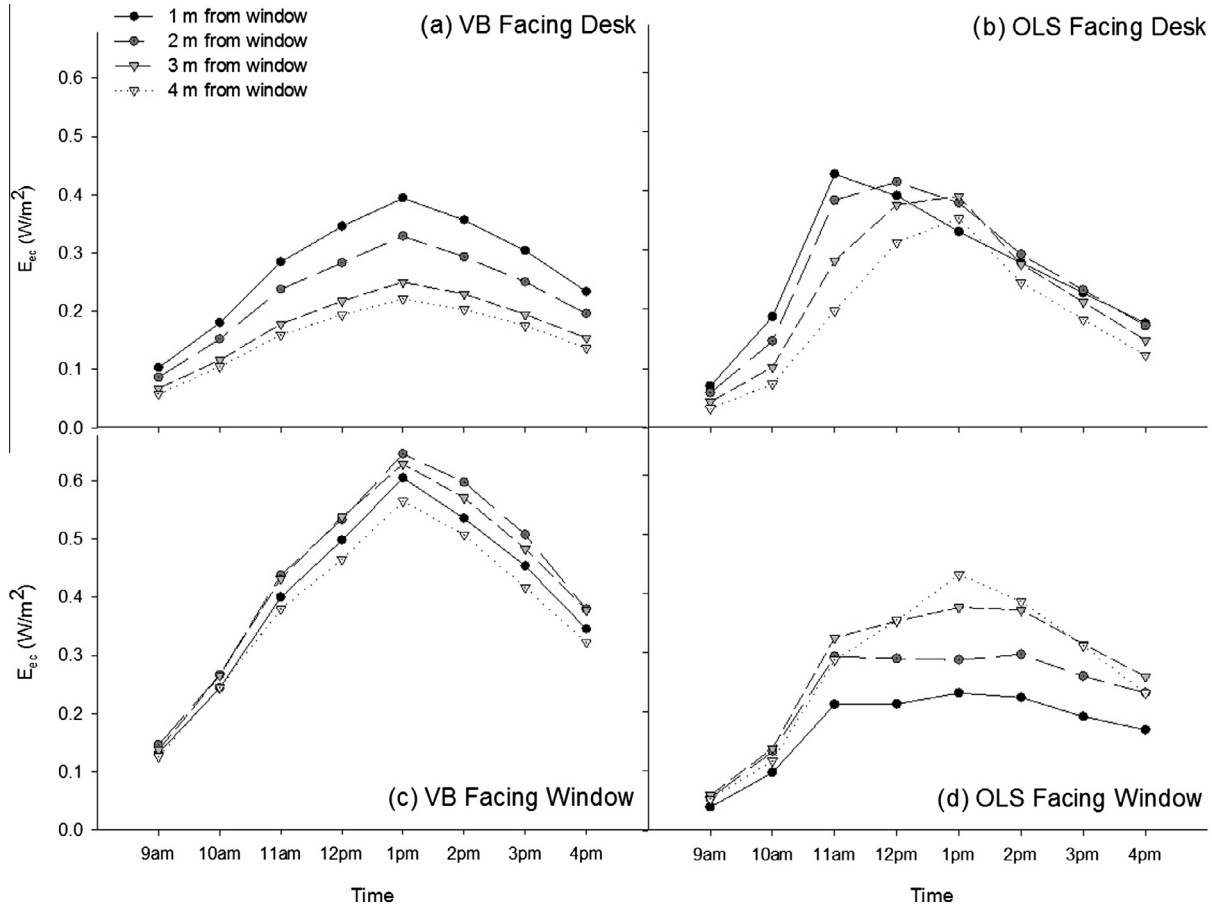

Fig. 8. Simulated circadian weighted irradiance E_{ec} (W/m^2) for different times: (a) Room I with VB facing the desk; (b) Room II equipped with OLS facing the desk; (c) Room I with VB facing the window and (d) Room II with OLS facing the window.

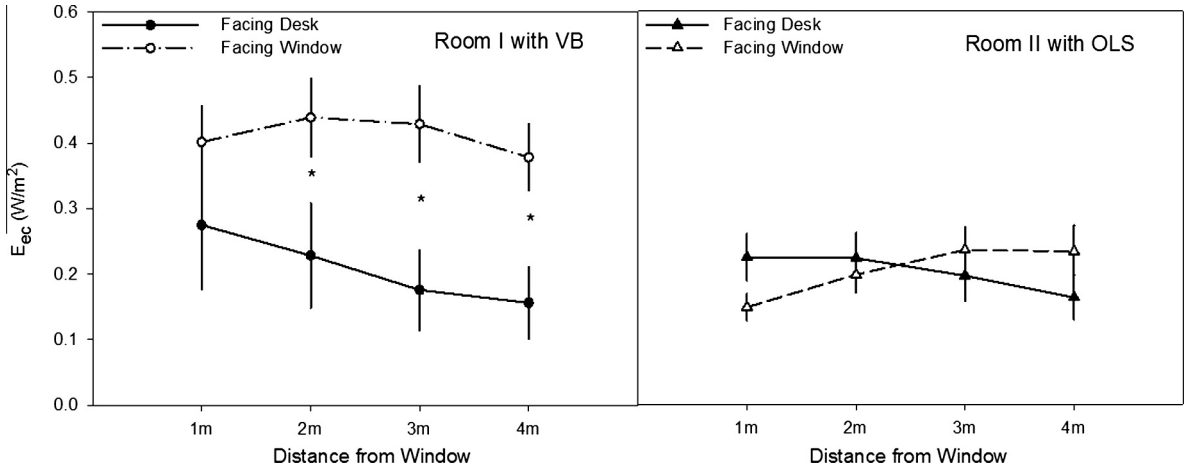

Fig. 9. Comparisons of simulated circadian irradiance [E_{ec} (W/m^2)] between (a) Room I with VB facing the desk (solid lines) and window (dashed lines); (b) Room II equipped with OLS facing the desk and window (means for eight time points ± SEM; $^* = p < 0.05$).

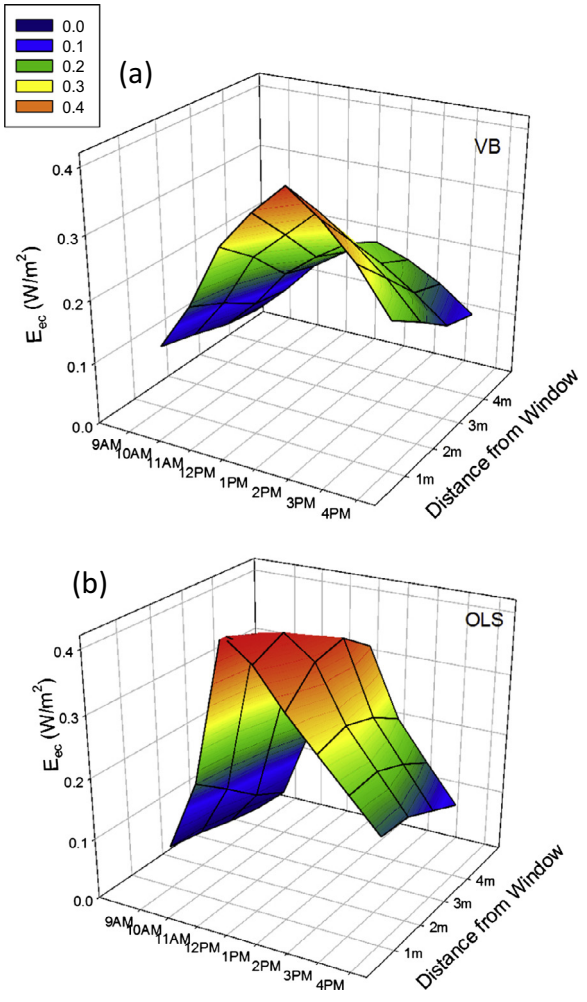

Fig. 10. The 3D mesh plots of simulated circadian weighted irradiance E_{ec} shown for different times and distances from the window for a virtual seated observer facing the desk (a) in Room I with VB and (b) in Room II with OLS. Warm colours (yellow-red) indicate higher and more bluish colours lower circadian weighted irradiance. For interpretation of the references to colour in this figure legend, the reader is referred to the web version of this article.

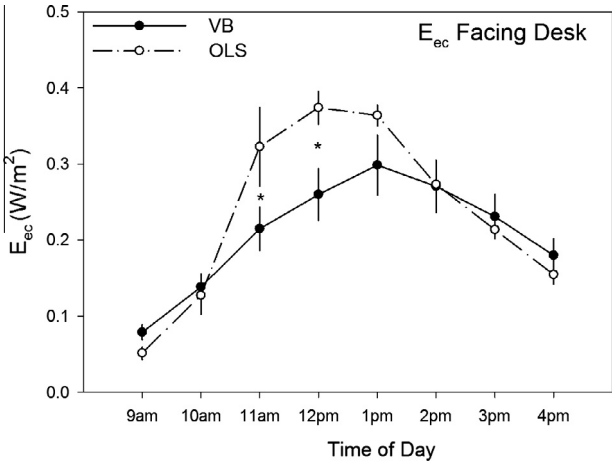

Fig. 11. Comparisons of E_{ec} simulated values for both rooms with VB and OLS for a seated virtual observer facing the desk in the course of a working day (9 AM–4 PM; $^* = p < 0.05$; main effect of 'daylighting system'; mean ± standard mean of error).

of 'time' × 'condition'; $p = 0.02$; Duncan's multiple range test).

4. Discussion

The lighting simulations carried out with RADIANCE provided illuminance and luminance distributions in the two test rooms that are comparable to those obtained by monitoring with a photometric equipment and with the Camera-Like Light Sensor (CLLS) based on a High Dynamic Range (HDR) vision sensor. Overall higher illuminance was found in the room equipped with VB compared to the room with OLS. The false colour images of these photometric variables obtained from simulation and CLLS monitoring in the rooms showed different luminance distributions over time for both daylight-redirecting systems: VB provided larger luminance on the horizontal

and vertical planes nearby the window, while the OLS provided larger luminance on the planes located in the room depth. The luminance ratio in-between the task areas and the adjacent walls showed reasonable values for both rooms. After a successful empirical validation of the simulations, the models were used for simulations of circadian metrics. The simulations produced distributions of circadian weighted radiance that were visually similar to those monitored with the CLLS. Interestingly, in the room with VB, the simulated E_{ec} was larger for a seated virtual observer facing the window, when compared to a virtual observer facing the desk. In the same test room, the results showed a decrease of simulated E_{ec} in the depth of the room after a distance of two metres away from the window. On the other hand, the room with OLS provided larger E_{ec} from 11 AM to 12 PM when compared to the room with VB (for a virtual observer seated facing the desk).

The simulation provided overall slightly higher luminance for both daylight-redirecting systems compared to the CLLS monitoring. Building up a precise virtual model for lighting simulation remains however a challenge due to the difficulties to handle with material reflectance and transmission, sky luminance distribution as well as software parameters (Mardaljevic, 1999; Thanachareonkit, 2008). In this case, the surface reflectance (ceilings, walls and floors) was spectrally neutral and the window glazing used for the simulation was approximately equivalent to the real one; these might cause only some minor errors in computation. Moreover, two difficulties inherent to daylighting simulation were previously addressed: the ability to measure Bi-directional Scattering Density Functions (BSDF data) of complex fenestration systems as well as the ability to reproduce the precise daylighting conditions (such as climate and orientation) in computer simulations (McNeil and Lee, 2013). Particularly, photometric variables depend on the red and green channels; our RGB approximation method might impact on the luminance value. Furthermore, the sky luminance distributions used in this study and generated by the *gensky* command, is based on CIE standard sky models. In reality, there might be some changes of the sky luminance distribution over time that the simulations cannot precisely reproduce.

The current study did not use *a proxy* to evaluate the photo-biological effects of daylight, as it was done in other studies: we investigated absolute values of the circadian weighted radiance (L_{ec}) and irradiance (E_{ec}) by the way of on-site monitoring and computer rendering. Besides the use of the L_{ec} distribution for comparisons with the CLLS monitoring, the absolute E_{ec} values determined by simulation can contribute to create a 'dose–response curve' of light exposure related to alertness and well-being at different times of day. The circadian weighted irradiance as it is used in this study reflects absolute sensitivity of ipRGCs and does not integrate the sensitivity of the circadian system at different times of day. Linhart et al. (2013) compared a static blue-enriched polychromatic white light source (17 000 K) in an office with daylighting conditions under overcast, intermediate and clear skies. They found that circadian weighted irradiance (E_{ec}) reached 0.5 W/m^2 with blue-enrich polychromatic white light for a potential seated observer, which was always lower than daylight except early in the morning and in the evenings and under an overcast sky. In the current study, the E_{ec} values at eye level did not reach 0.5 W/m^2 throughout the day for a seated observer facing a desk even under a clear sky, while it reached 0.4 W/m^2 in the room equipped with VB from 11 AM to 3 PM, for an observer facing the southern window. Hence, those individual daylighting systems at the upper part of the window might not provide adequate light flux to evoke strong non-visual effects – at least not on a day where light levels are low.

Nonetheless, it has to be outlined that the daylighting systems were installed above a conventional window, covered with opaque screens. The present results point out accordingly only the specific photo-biological effects of the daylight-redirecting systems. In a realistic situation, there should be more openings underneath the daylighting systems providing more daylight and outside view, except when the openings are fully shaded. The present experiment must be considered as a simple case-study allowing a quantitative evaluation of the photo-biological impact of daylight. Future studies in basic (and recommendations for an optimal 'light dose' which could be assessed in circadian metrics at different times of day a good estimate. This would support prediction of alertness, well-being and working performance of building occupants. A recent publication authored by many experts in the field outlined the need for a new metric to include biological effects also in architectural settings (Lucas et al., 2014).

The monitored data showed higher illuminance provided by the venetian blinds throughout the day compared to optical louver systems. However, the results showed larger circadian weighted irradiance for OLS compared to VB at 11AM and 12 PM. This implies that circadian weight irradiance might not always proportional to illuminance. The circadian metric can be influenced by the spectral composition of light, which might be changed due to the materials or the re-direction of daylighting systems, as it was recently recommended (Andersen, 2015).

5. Conclusion

Our results indicated that different locations within the two test rooms provided different circadian metrics. It appears that the circadian irradiance is related to the photopic illuminance, however, the circadian metric is not always proportional to the photometric one. Using computer simulation will aid to predict the impact of light on non-visual functions. During the design process, the simulation of the photo-biological aspects of daylight can be performed for different sky and electric lighting conditions at any time of the year and any geographical location. Nonetheless, the RGB approximation is a convenient method to calculate both photopic and circadian metrics.

In a next step, computer simulations of circadian metrics might be compared with physical monitoring, carried out with a spectroradiometer, in order to validate precisely the simulation model. Daylighting strategies would be easier and more accurate to implement in practice and to provide valuable recommendations regarding the photobiological impact of light on human physiology and behaviour.

Acknowledgements

The authors thank the Lawrence Berkeley National Laboratory (USA), especially Eleanor Lee for inviting and hosting the first author and Dr Andrew McNeil for the virtual models of the testrooms. The authors are grateful to the Centre Suisse d'Electronique et de Microtechnique (CSEM, Switzerland) for their collaboration (especially Dr. Ségolène Pangaud and Dr. Edo Franzi). We would like also to thank Pierre Loesch (LESO-PB EPFL) for technical support. The work was financially supported by the Velux Foundation (Switzerland) as well as a PhD mobility award from the EDCE doctoral school (EPFL, Switzerland).

References

Andersen, M., 2015. Unweaving the human response in daylighting design. Build. Environ. 91, 101–117.

Andersen, M., Mardaljevic, J., Lockley, S.W., 2011. A framework for predicting non-visual effects of daylight: part I – photobiology-based model. Lighting Res. Technol. 44 (1), 37–53.

Andersen, M., Gochenour, S.J., Lockley, S.W., 2013. Modelling 'non-visual' effects of daylighting in a residential environment. Build. Environ. 70, 138–149.

Arm, C., et al., 2008. Icycam – a High Dynamic Range Vision System, in CSEM Scientific and Technical Report 2008, CSEM. p. 20.

Bellia, L., Bisegna, F., 2013. From radiometry to circadian photometry: a theoretical approach. Build. Environ. 62, 63–68.

Bierman, A., Klein, T.R., Rea, M.S., 2005. The Daysimeter: a device for measuring optical radiation as a stimulus for the human circadian system. Measur. Sci. Technol. 16 (11), 2292–2299.

Boff, K.R., Lincoln, J.E., 1988. In: Engineering Data Compendium. Human Perception and Performance, vol. 2. Wright-Patterson Air Force Base, Ohio.

Borisuit, A., 2013. The Impact of Light Including Non-Image Forming Effects on Visual Comfort. Ecole Polytechnique Fédérale de Lausanne (EPFL), Lausanne, Thesis # 6007.

Borisuit, A., Scartezzini, J.-L., Thanachareonkit, A., 2010. Visual comfort and glare risk assessment by HDR imaging technique. Arch. Sci. Rev. 53 (4), 359–373.

Borisuit, A., et al., 2012. A new device for dynamic luminance mapping and glare assessment in buildings. In: SPIE Optics+Photonics Conference 2012. San Diego.

Borisuit, A., et al., 2013. Assessment of circadian weighted radiance distribution using a camera-like light sensor. In: Proceedings of CISBAT 2013 International Scientific Conference. Lausanne, Switzerland.

Brainard, G.C. et al., 2001. Action spectrum for melatonin regulation in humans: evidence for a novel circadian photoreceptor. J. Neurosci. 21 (16), 6405–6412.

Cajochen, C., 2007. Alerting effects of light. Sleep Med. Rev. 11 (6), 453–464.

Cajochen, C. et al., 2005. High sensitivity of human melatonin, alertness, thermoregulation, and heart rate to short wavelength light. J. Clin. Endocrinol. Metab. 90 (3), 1311–1316.

Chellappa, S.L. et al., 2011. Non-visual effects of light on melatonin, alertness and cognitive performance: can blue-enriched light keep us alert?. PLoS One 6 (1) e16429.

Commission Internationale de l'Eclairage (CIE), 1978. Light as a true visual quantity: principles of measurement. In: CIE 041-1978. Commission international de l'éclairage, Vienna.

Commission Internationale de l'Eclairage (CIE), 2004. Ocular lighting effects on human physiology and behaviour. In: CIE Technical Support 158, C.I.d. l'Eclairage, Editor, CIE Vienna.

Czeisler, C.A. et al., 1986. Bright light resets the human circadian pacemaker independent of the timing of the sleep-wake cycle. Science 233 (4764), 667–671.

Figueiro, M. et al., 2013. Comparisons of three practical field devices used to measure personal light exposures and activity levels. Lighting Res. Technol. 45 (4), 421–434.

Foster, R.G., 1998. Shedding light on the biological clock. Neuron 20 (5), 829–832.

Gall, D., 2002. Circadiane Lichtgrössen und deren messtechnische Ermittlung (German). Licht 11–12, 1292–1297.

Gall, D., Bieske, K., 2004. Definition and measurement of circadian radiometric quantities. In: CIE Symposium 2004 on Light and Health: Non-Visual Effects. Commission internationale de l'éclairage, Vienna, Austria.

Gall, D., Lapuente, V., 2002. Beleuchtungsrelevante Aspekte bei der Auswahl eines förderlichen Lampenspektrums (German). Licht 54 (7), 860–871.

Geisler-Moroder, D., Dür, A., 2010. Estimating melatonin suppression and photosynthesis activity in real-world scenes from computer generated images. In: 5th European Conference on Colour in Graphics, Imaging, and Vision 2010. Joensuu, Finland, pp. 346–352.

Hubalek, S., Zöschg, D., Schierz, C., 2006. Ambulant recording of light for vision and non-visual biological effects. Lighting Res. Technol. 38 (4), 314–324.

Kämpf, J., Scartezzini, J., 2011. Ray-tracing simulation of complex fenestration systems based on digitally processed BTDF data. In: Proceedings of CISBAT 2011 International Scientific Conference. Lausanne, Switzerland.

Kozakov, R., Franke, S., Schöpp, H., 2008. Approach to an effective biological spectrum of a light source. LEUKOS – J. Illuminat. Eng. Soc. North America 4 (4), 255–263.

Larson, G.W., 1991. LUMFACTOR: Luminous Efficacy changed from 470 to 179. In: RADIANCE Digest.

Larson, G.W., Shakespeare, R.A., 1998. Rendering with Radiance: The Art and Science of Lighting Visualization. Morgan Kaufmann Publishers, San Francisco, CA.

LBNL. *WINDOW 7.2*. WINDOW Software 2014 [cited 2014 March, 15]; <http://windows.lbl.gov/software/window/window.html>.

Lewy, A.J. et al., 1980. Light suppresses melatonin secretion in humans. Science 210 (4475), 1267–1269.

Linhart, F., Scartezzini, J.-L., Münch, M., 2009. Daylight exposure and circadian efficiency in office rooms equipped with anidolic daylighting systems. In: Proceedings of CISBAT 2013 International Scientific Conference. Lausanne, Switzerland.

Lucas, R.J., Douglas, R.H., Foster, R.G., 2001. Characterization of an ocular photopigment capable of driving pupillary constriction in mice. Nat. Neurosci. 4 (6), 621–626.

Lucas, R., Peirson, S., Berson, D., Brown, T., Cooper, H., Czeisler, C., Figueiro, M., Gamlin, P., Lockley, S., O'Hagan, J., Price, L., Provencio, I., Skene, D., Brainard, G., 2014. Measuring and using light in the melanopsin age. Trends Neurosci. 37 (1), 1–9.

Maamari, F. et al., 2003. Reliable datasets for lighting programs validation – benchmark results. Solar Energy 79 (2), 213–215.

Mardaljevic, J., 1999. Daylight Simulation: Validation, Sky Models and Daylight Coefficients. De Montfort University, Leicester (UK).

McNeil, A., Lee, E.S., 2013. A validation of the Radiance three-phase simulation method for modeling annual daylight performance of optically complex fenestration systems. J. Build. Perform. Simul. 6 (1), 24–37.

Münch, M., Bromundt, V., 2012. Light and chronobiology: implications for health and disease. Dialogues Clin. Neurosci. 14 (4), 448–453.

Münch, M. et al., 2012. Effects of prior light exposure on early evening performance, subjective sleepiness, and hormonal secretion. Behav. Neurosci. 126 (1), 196–203.

Nabil, A., Mardaljevic, J., 2005. Useful daylight illuminance: a new paradigm for assessing daylight in buildings. Lighting Res. Technol. 37 (1), 41–59.

Pangaud, S., 2011. Description de la télémétrie de l'application embarquée ů viewer v3.5b ý, DEVISE-IcyCAM VSLOG. Centre Suisse d'électronique et de microtechnique (CSEM), Neuchâtel.

Pechacek, C.S., Andersen, M., Lockley, S.W., 2008. Preliminary method for prospective analysis of the circadian efficacy of (day)light with applications to healthcare architecture. LEUKOS – J. Illuminat. Eng. Soc. North America 5 (1), 1–26.

Rea, M.S., 2000. IESNA Lighting Handbook: Reference & Application the, 9th ed. Illuminating Engineering Society of North America, New York.

Rea, M.S., 2002. Phototransduction for human melatonin suppression. J. Pineal Res. 32 (4), 209–213.

Rea, M.S. et al., 2008. A new approach to understanding the impact of circadian disruption on human health. J. Circadian Rhythms 6, 7.

Reinhart, C.F., Herkel, S., 2000. The simulation of annual daylight illuminance distributions – a state-of-the-art comparison of six RADIANCE-based methods. Energy Build. 32 (2), 167–187.

Roulet, C., 2008. Santé et qualité de l'environnement intérieur dans les bâtiments (French), second ed. PPUR presses polytechniques.

Thanachareonkit, A., 2008. Comparing Physical and Virtual Methods for Daylight Performance Modelling Including Complex Fenestration Systems. Ecole Polytechnique Federale de Lausanne, Lausanne (Switzerland).

Thanachareonkit, A., Lee, E.S., McNeil, A., 2013. Empirical assessment of a prismatic daylight redirecting window film in a full-scale office testbed. Leukos 10 (1), 19–45.

Thapan, K., Arendt, J., Skene, D.J., 2001. An action spectrum for melatonin suppression: evidence for a novel non-rod, non-cone photoreceptor system in humans. J. Physiol. 535 (1), 261–267.

Ulbricht, C., Wilkie, A., Purgathofer, W., 2005. Verification of physically based rendering algorithms. Comput. Graphics Forum 25 (2), 237–255.

Ward, G. et al., 2011. Simulating the daylight performance of complex fenestration systems using bidirectional scattering distribution functions within Radiance. Leukos 7 (4), 241–261.

Wirz-Justice, A., Fournier, C., 2010. Light, health and wellbeing: implications from chronobiology for architectural design. World Health Des. 8, 44–49.